Magnetic behaviour of the doped antiferromagnet $K_2Fe_{1-x}Ga_xF_5$

1989 J. Phys.: Condens. Matter 1 6731

(http://iopscience.iop.org/0953-8984/1/37/019)

J. Phys.: Condens. Matter 1 (1989) 6731–6744. Printed in the UK

Magnetic behaviour of the doped antiferromagnet $K_2Fe_{1-x}Ga_xF_5$

J Chadwick, D H Jones, J A Johnson, C E Johnson and M F Thomas
Department of Physics, University of Liverpool, Liverpool L69 3BX, UK

Received 6 December 1988

Abstract. The mixed fluorides $K_2Fe_{1-x}Ga_xF_5$ are quasi-one-dimensional antiferromagnets in which the chains of Fe^{3+} ions are segmented by doping with non-magnetic Ga^{3+} ions. Mössbauer spectra of samples with doping level $x = 0.008, 0.01, 0.017, 0.027, 0.037, 0.062, 0.079$ and 0.095 were analysed to provide information on the different excitation modes of doped and undoped material, the variation of the three-dimensional ordering temperature T_N on x and the spin-flop transition in the doped material. The results are compared with a model in which segments of magnetic chains relax within the molecular field of the whole sample.

1. Introduction

The pure antiferromagnet K_2FeF_5 has a quasi-one-dimensional magnetic structure having a three-dimensional ordering temperature $T_N = 6.95$ K (Cooper *et al* 1982a). This structure is composed of chains of Fe^{3+} ions coupled by superexchange via the intervening F^- ions. The intrachain interaction is specified by a coupling constant J. The chains are separated by the K^+ ions such that superexchange interaction between the chains, specified by a coupling constant J', is much weaker than the intrachain interaction. A number of studies by means of magnetic susceptibility, neutron diffraction and Mössbauer spectroscopy (Dance *et al* 1980, Gupta *et al* 1978, Cooper *et al* 1982a, b) have determined the ratio of J'/J to be 9×10^{-4} and have obtained evidence that spin correlation within the chains persists to temperatures of about 100 K.

The aim of the present study is to investigate the effect on the magnetic properties of doping non-magnetic Ga^{3+} ions into the material. The Ga^{3+} ions substitute for the Fe^{3+} ions segmenting the magnetically coupled chains. A schematic representation of the expected magnetic structure of the doped compound at a temperature $T < T_N$ is shown in figure 1. In particular we wish to study the effect of the level of Ga^{3+} doping, x, on the ordering temperature T_N and on relaxation effects associated with the fluctuation of the chain segments.

2. Experimental Technique

Spectra were taken with a conventional Mössbauer spectrometer running in the constant acceleration mode using sources of ^{57}Co in rhodium. Power samples for all values of x were made from small crystals crushed and mixed with boron nitride to give evenly

0953-8984/89/376731 + 14 $02.50

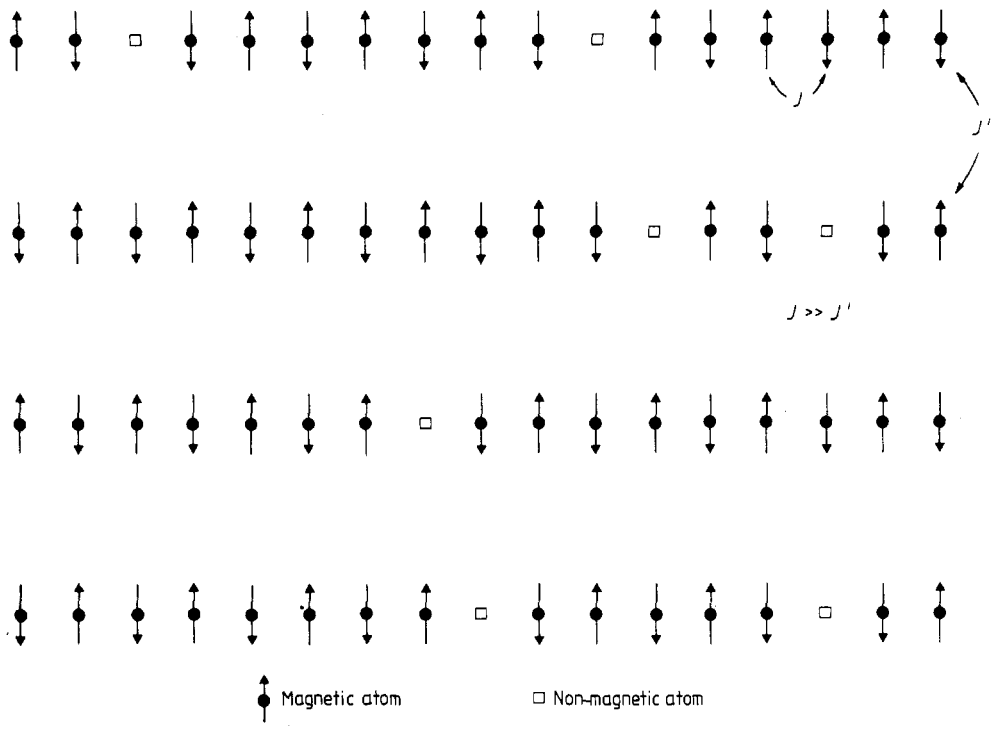

Figure 1. Schematic magnetic structure of K_2FeF_5 doped with gallium.

spread absorbers of thickness about 5 mg of iron cm^{-2}. The single-crystal samples of $K_2Fe_{0.99}Ga_{0.01}F_5$ was oriented by Laue x-ray diffraction and reduced by careful abrasion to give optimum thickness with the crystalline *b* axis (the antiferromagnetic axis) normal to the plane of the sample.

Temperatures in the range 1.3–4.2 K were achieved by pumping on a bath of liquid helium in which the sample was immersed. For temperatures in the range 4.2–10 K the sample was mounted in an evacuated insert immersed in a helium bath. A carbon glass resistor measured the temperature and acted as a sensor to stabilise the temperature via a resistance bridge and heating coil control. The temperature stability over the normal counting time of a few hours was better than 0.05 K.

Magnetic fields of up to 10 T were generated by a Helmholtz pair of superconducting coils at the sample position. At the source position zero field was achieved by means of a reverse-wound bucking coil which cancelled the field of the main coils. In the series of spectra illustrating spin flop the single-crystal sample was mounted with the *b* axis parallel to the magnetic field and the direction of the gamma-ray beam. In this configuration the source was mounted at the end of a vertical drive rod and was immersed in the helium bath. For the control experiments with the magnetic field applied along the crystal *a* or *c* axes the magnetic field was in the plane of the absorber and the gamma-ray beam was directed between the Helmholtz coils from a source at room temperature.

3. Results and analysis

3.1. Polycrystalline samples

Typical series of spectra taken for a range of low temperatures and at room temperature are shown in figures 2, 3 and 4 for doping levels $x = 0.008$, 0.037 and 0.079 respectively.

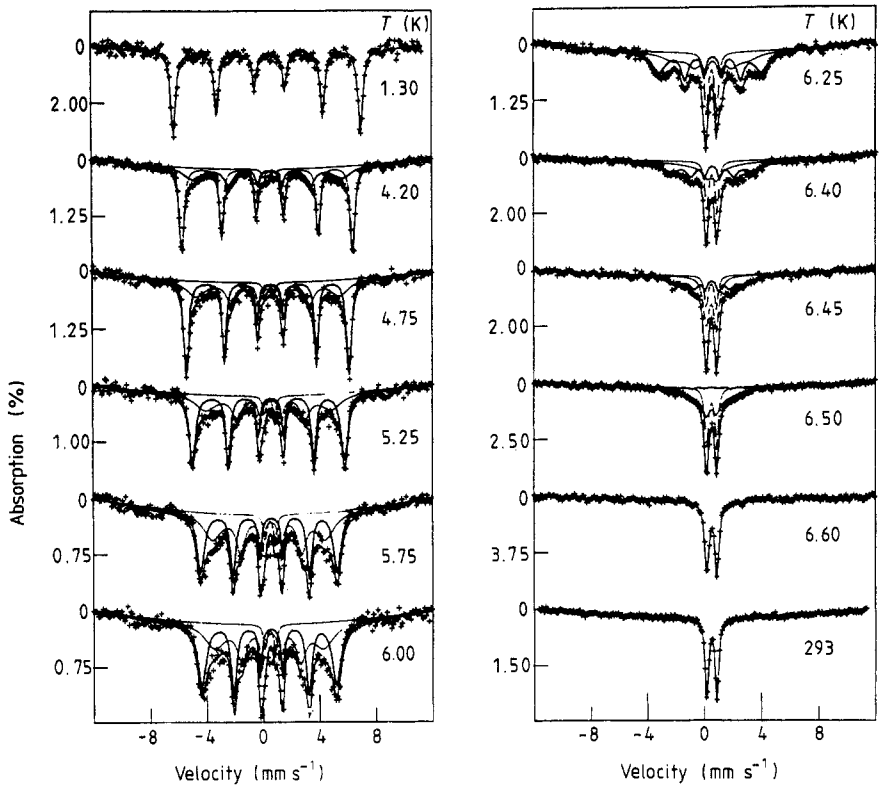

Figure 2. Series of spectra showing the variation with temperature of a powder sample of $K_2Fe_{1-x}Ga_xF_5$ with $x = 0.008$. The computer fits to the spectra are discussed in § 3.1 and the values of the parameters listed in table 1.

The development of the shape of the spectra with increasing temperature goes through the stages of a sextet of sharp lines, broadened sextet, doublet with broadly distributed magnetic component to a doublet of sharp lines.

In adopting a framework for fitting spectra with magnetic components two alternative approaches arise: (i) a distribution of hyperfine fields $P(B_{hf})$; or (ii) relaxation in which more than one relaxation time is needed. The better fits to the spectra were obtained with the latter approach. The model of magnetic structure to be discussed in the next section also inclined us toward the latter approach, and fits to all the spectra shown in figures 2–4 were based upon up to three components: two magnetic with different relaxation rates and a non-magnetic quadrupole doublet. Relaxation of the magnetic ions was represented by the standard two-level model of Blume and Tjon (1968) with splitting of the levels representing the molecular field of the ordered sample on the relaxing ions. The relaxation analysis applied to the temperature dependence of the spectra of the polycrystalline samples differed in detail from that applied to the spin-flop spectra because we wished to highlight different parameters in the two cases.

For the evolution of the spectra of the polycrystalline samples with temperature a quantity of interest was the relative sublattice magnetisation M which is equivalent to the magnetic moment per magnetic ion. This is given by

$$M = (P_1 - P_2)/(P_1 + P_2)$$

where P_1 and P_2 are the populations of the lower and upper magnetic states of the ion.

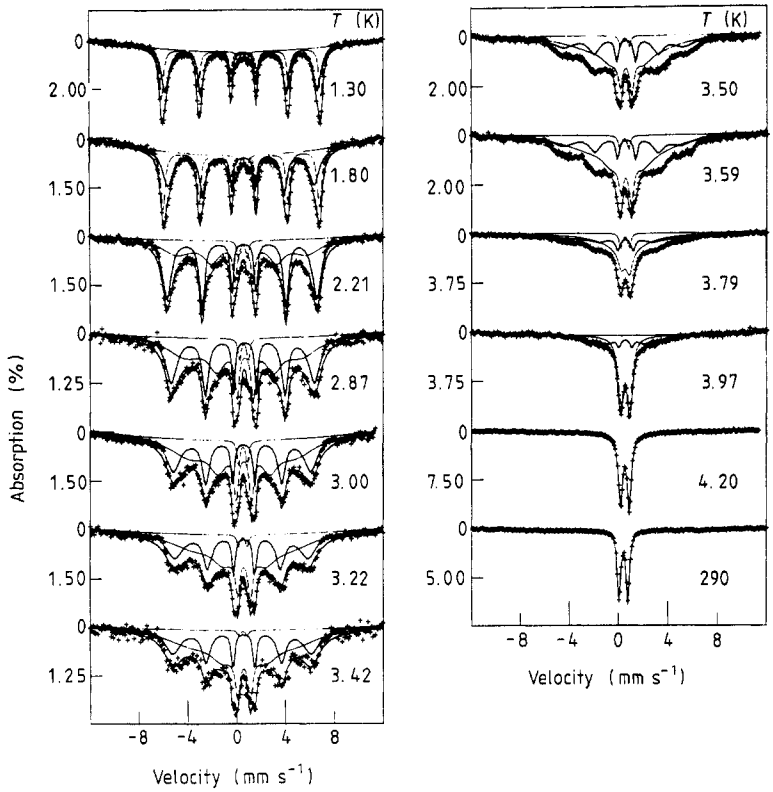

Figure 3. Series of spectra showing the variation with temperature of a powder sample of $K_2Fe_{1-x}Ga_xF_5$ with $x = 0.037$. The fits to the spectra are computed in the manner discussed in § 3.1.

In the fits to the polycrystalline spectra, some of which are shown in figures 2–4 the magnitude of the fluctuating hyperfine field was kept constant at the saturation value for K_2FeF_5; $B_{hf}(sat) = 41.0$ T. The sharp sextet component is generated by fast fluctuation of the magnetic ions (within segment) which generates an effective hyperfine field which is scaled by M. The broader sextet occurs when segment fluctuation times t enter the range $0.2 \times 10^{-9}\,s < t < 10 \times 10^{-9}\,s$, comparable to the hyperfine sensing time. The quadrupole doublet component arises from fast fluctuating ions not subject to a molecular field. It is seen that this component has negligible intensity until temperatures close to the ordering temperature where local inhomogeneities may leave some regions in zero molecular field. Figures 2–4 show that good fits to all the spectra can be obtained using this approach. Details of the transition rates, magnetisations M and relative areas of components for the spectra shown in figure 2 are listed in table 1.

3.2. Determination of T_N and variation of T_N with x

Relaxation occurs between two states of the magnetic ion whose energy splitting is proportional to the field acting at the relaxing ion. Identifying this field with the molecular field produced by the magnetically ordered material a measure of the relative sublattice magnetisation M is obtained from the analysis.

Splitting of the states and hence the relative magnetisation M disappears at the ordering temperature, giving a sensitive method of determining T_N from the fits to the

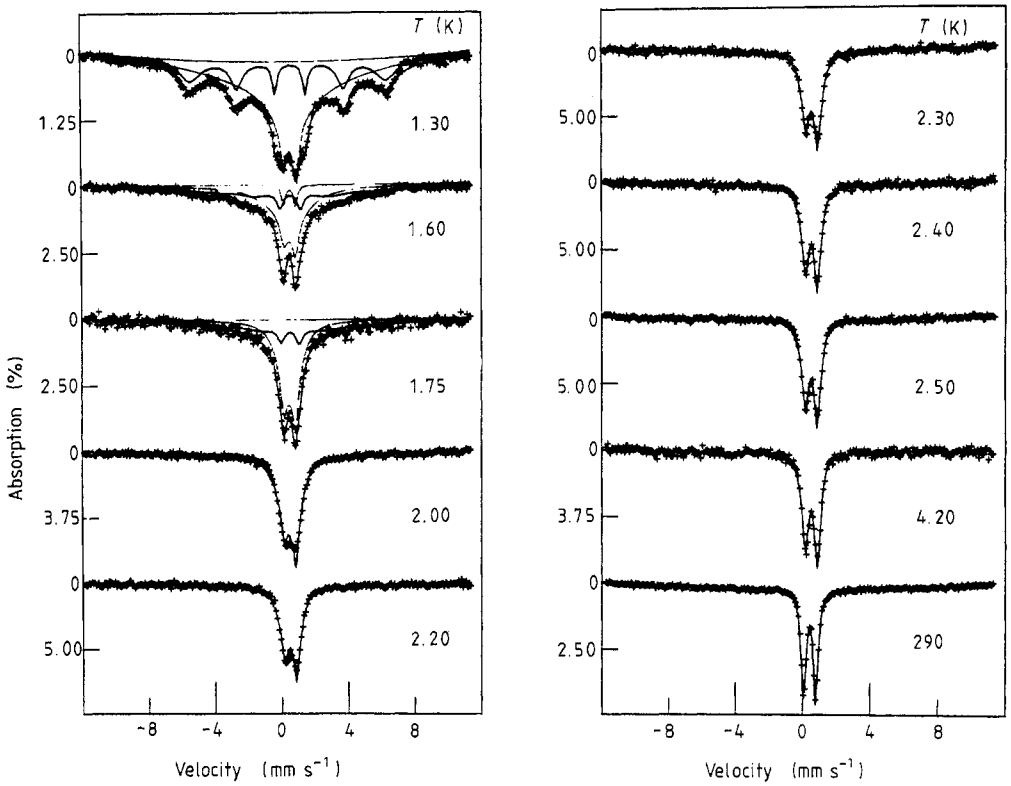

Figure 4. Series of spectra showing the variation with temperature of a powder sample of $K_2Fe_{1-x}Ga_xF_5$ with $x = 0.079$. The fits to the spectra are computed in the manner discussed in § 3.1.

Table 1. Transition rates, relative magnetisations M and relative areas of the components of the fits to the spectra of a polycrystalline sample of $K_2Fe_{1-x}Ga_xF_5$ ($x = 0.008$) are listed as a function of temperature. The spectra are shown in figure 2. For each magnetic component the fluctuating hyperfine field was fixed at $B_{hf} = 41.0$ T. Values of the relative magnetisations M for component 1 are plotted in figure 5.

	Component 1			Component 2			Doublet component
Temperature (K)	Transition time (10^{-9} s)	M	Area (%)	Transition time (10^{-9} s)	M	Area (%)	Area (%)
1.3	1.0	0.98	100				
4.2	0.08	0.90	63	0.53	0.76	35	3
4.75	0.07	0.86	58	0.55	0.73	40	2
5.25	0.13	0.80	56	0.50	0.64	40	4
5.75	0.14	0.72	47	0.39	0.58	48	5
6.0	0.17	0.71	51	0.45	0.55	45	4
6.25	0.25	0.53	47	0.51	0.35	34	19
6.4	0.35	0.41	45	1.33	0.0	32	23
6.45	0.32	0.35	42	0.11	0.0	41	17
6.5	0.06	0.38	5	0.71	0.13	60	35
6.6				0.04	0.0	100	
293				0.003	0.0	100	

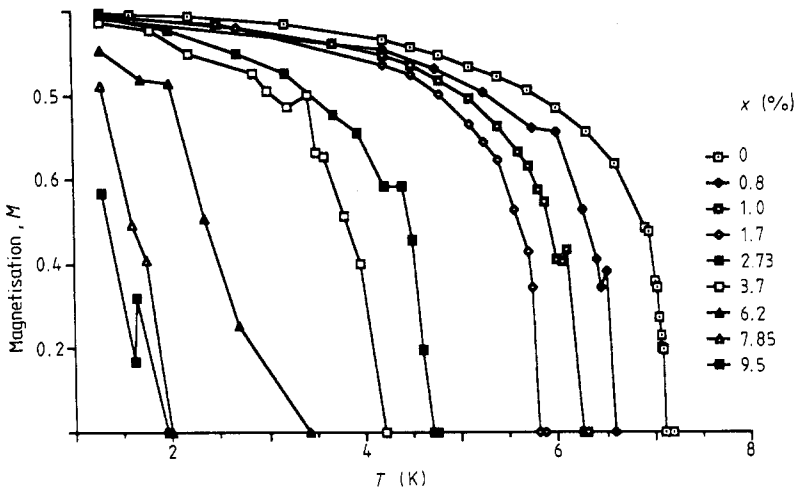

Figure 5. Variation of magnetisation M (defined in the text) with temperature T for $K_2Fe_{1-x}Ga_xF_5$ samples with different levels of doping x expressed as a percentage. The curves through the points are to guide the eye.

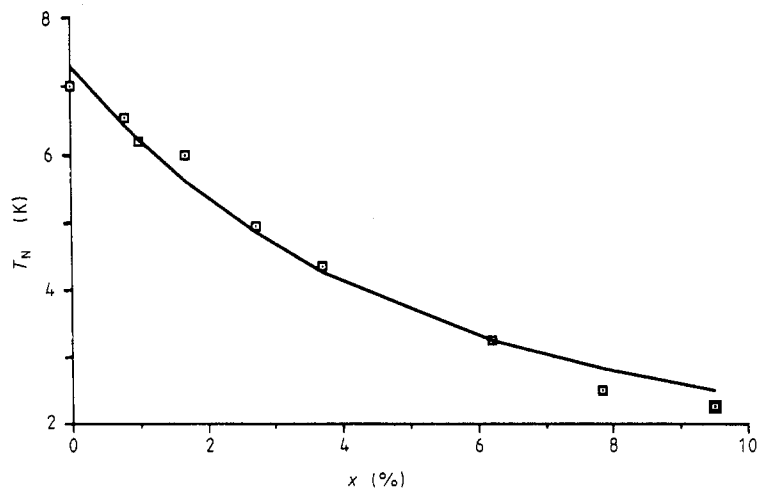

Figure 6. Variation of ordering temperatures T_N from figure 5 with doping level x. The doping level is expressed as a percentage. The fit to the data is given by equation (5) of § 4.3.

spectra. The results of this procedure are shown in figure 5 where the values of relative magnetisation M for component 1 of table 1 are plotted against temperature T for all the samples studied. It is seen that for samples with doping levels $x < 0.037$, where data from a large number of spectra can be included, the procedure gave convincing variation of M versus T curves and fixed precise values for T_N. For the samples with doping levels $x = 0.062$, 0.079 and 0.095 the data were more scanty and the values of T_N less precise. The values of $T_N(x)$ versus x are plotted in figure 6 and compared to the predictions of the model discussed in the next section.

3.3. Spin flop in a single-crystal sample

The spin-flop transition consists of a reorientation of the antiferromagnetic axis from the crystal b axis into the crystal ac plane under the influence of a field B of sufficient

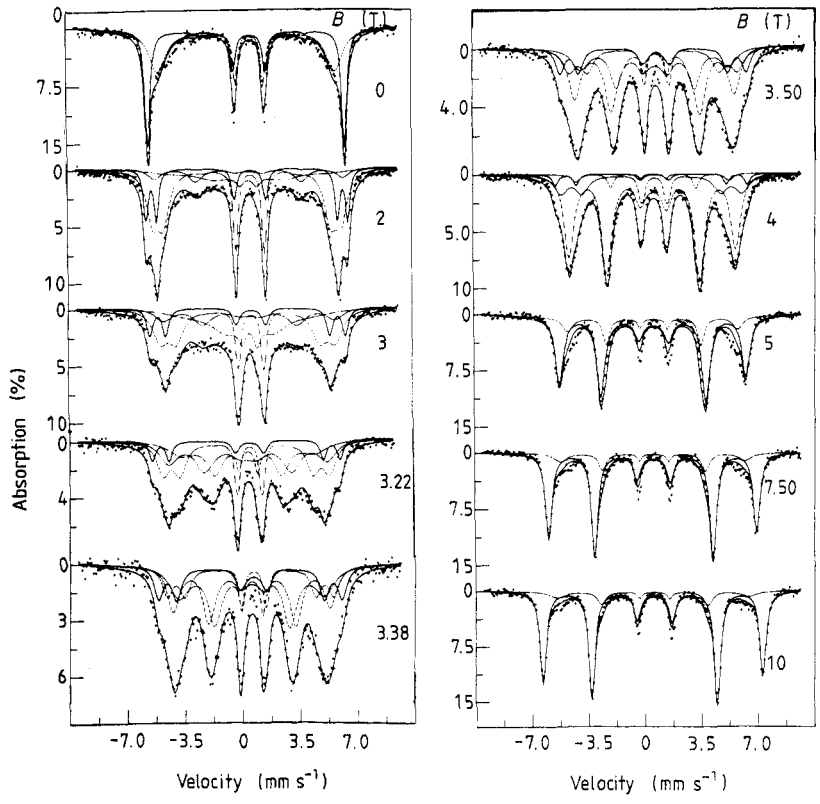

Figure 7. Series of spectra taken at 4.2 K with field B along the crystal b axis (antiferromagnetic axis) showing spin flop with extreme line broadening in a single crystal of $K_2Fe_{0.99}Ga_{0.01}F_5$. The computer fits to the spectra are discussed in § 3.3 and the values of the parameters listed in table 2.

strength applied along the antiferromagnetic easy axis. A series of spectra of the spin-flop transition in a single-crystal sample of $K_2Fe_{0.99}Ga_{0.01}F_5$ is shown in figure 7. With the magnetic field and gamma-ray beam both directed along the b axis the unflopped antiferromagnetic phase is characterised by an area ratio of 3 : 0 : 1 for the outer, middle and inner pairs of lines of the magnetic sextet. These lines split as the applied field B adds to and subtracts from the antiferromagnetic sublattices. The spin-flop phase in which the spins lie normal to the gamma-ray direction is characterised by an area ratio of 3 : 4 : 1 and unsplit lines. Thus the spin-flop transition is marked by the appearance of the middle ($\Delta m = 0$) pair of lines at or near the critical spin-flop field $B = B_{sf}$. In contrast to the spectra illustrating spin flop in pure K_2FeF_5 where, although some line broadening occurs at spin flop (Pankhurst *et al* 1985) it is not pronounced and is limited to fields within 0.1 T of B_{sf}, the spectra for $K_2Fe_{0.99}Ga_{0.01}F_5$ show pronounced line broadening throughout the range $2 < B < 4$ T. In fitting the series of spectra the model of relaxing segments of magnetic chain, used in the interpretation of the powder spectra, was applied. In the region of spin flop the applied field acts to cancel the crystalline anisotropy of the iron spins. The resultant weakened anisotropy acting near the transition results in enhanced fluctuations of the chain segments causing the relaxation broadening observed in the spectra. Accordingly in the series of spectra spanning the spin flop all spectra are fitted with relaxing components for the antiferromagnetic and spin-flop

phases. At applied fields $B \ll B_{sf}$ only the antiferromagnetic components contribute to the fit but for $B \simeq B_{sf}$ sharp and broadened components from the spin-flop phase are included. For values of $B > B_{sf}$ the spin-flop components predominate and for fields $B=$ 5, 7.5 and 10.0 T the sharp spin-flop component dominates the fits.

The relaxation analysis for these spectra differs in detail from that for the polycrystalline samples. In the series of spectra illustrating the spin flop, the sharp components of the antiferromagnetic and spin-flop phases are represented by slowly relaxing segments with hyperfine field values that are fixed by the fit. For each magnetic phase the same hyperfine field applies to both components. This method of analysis is adopted to highlight the variation of hyperfine field through the spin-flop transition. This is in line with previous analysis of spin flop in pure K_2FeF_5 (Gupta *et al* 1979). The values of the hyperfine field values for both phases are plotted against applied field in figure 10 below. The transition rates, values of hyperfine field, relative magnetisations and relative areas of components for the fits to the spectra shown in figure 7 are listed in table 2. For long relaxation times of greater than 10×10^{-9} s the magnetic sextet components of the antiferromagnetic and spin flop phases are completely insensitive to the relative magnetisation M.

The model implicit in the fits ascribes the spectral broadening near spin flop to the reduction in net anisotropy caused by the external field applied along the antiferromagnetic (crystal b) axis. No such broadening is expected if the field is applied along the crystal a or c axes. In order to test this prediction a series of spectra was taken with similar ranges of field applied along these axes. The results for both axes are similar and are illustrated for B along the c axis in figure 8. In these experiments the gamma-ray beam was along the crystal b axis—the axis of the antiferromagnetic spins. The spectra show that no spin reorientation occurs and that the line broadening evident at zero applied field is even somewhat reduced as the applied field is increased. This is in agreement with the model as in this geometry the applied field acts to enhance the crystalline anisotropy.

Spectra taken with the applied field B successively increasing and decreasing through the spin-flop region show hysteresis. It is seen in figure 9 that spectra at fields $B = 3.25$ and 3.32 T show different intensities of the middle ($\Delta m = 0$) pair of lines according to whether the field applied is in an increasing or decreasing series. The hysteresis is observed in the range of applied field $3.19 < B < 3.38$ T.

Although the most noticeable feature of spectra illustrating spin flop is the intensity of the middle pair of lines, the most precise measurement of the spin-flop field B_{sf} is given by the minimum in the value of the hyperfine field B_{hf} as a function of applied field B. The variation of B_{hf} versus B is shown in figure 10 where the values of B_{hf} for the components of the antiferromagnetic and spin-flop phases are shown and compared with those of pure K_2FeF_5. These minima determine a value of the spin-flop field for $K_2Fe_{0.99}Ga_{0.01}F_5$ as $B_{sf}(x = 0.01) = 3.40 \pm 0.1$ T compared to that of pure K_2FeF_5 where $B_{sf}(0) = 3.65 \pm 0.1$ T (Pankhurst *et al* 1985).

4. Discussion

4.1. Magnetic model of $K_2Fe_{1-x}Ga_xF_5$

Previous Mössbauer studies (Gupta *et al* 1979, Cooper *et al* 1982a, b, Pankhurst *et al* 1985) have shown that K_2FeF_5 behaves as a quasi-one-dimensional antiferromagnet with weak interchain coupling J' and strong intrachain coupling J. The ratio of coupling

Table 2. Transition rates, hyperfine fields, relative magnetisations M and relative areas of the components of the fits to the spectra of a single-crystal sample of $K_2Fe_{1-x}Ga_xF_5$ ($x = 0.01$) are listed as a function of field applied along the antiferromagnetic b axis. The spectra are shown in figure 7. The magnitudes of the hyperfine fields are plotted in figure 10. For relaxation times greater than 10×10^{-9} s the spectra are insensitive to the relative magnetisation M.

	Antiferromagnetic phase						Spin-flop phase					
	Component 1			Component 2			Component 1			Component 2		
Applied field (T)	Transition time (10^{-9} s)	B_{hf} (T)	Area (%)	Transition time (10^{-9} s)	M	Area (%)	Transition time (10^{-9} s)	B_{hf} (T)	Area (%)	Transition time (10^{-9} s)	M	Area (%)
0	350	36.8	47	1.0	0.85	53						
2.0	577	35.8	20	1.0	0.89	50	40	35.4	11	3.2	0.42	19
3.0	179	33.7	14	1.0	0.84	39	27	32.3	18	2.2	0.39	29
3.22	162	33.0	10	0.8	0.84	32	24	30.8	31	1.8	0.67	27
3.38	73	31.5	18	0.7	0.87	18	45	29.7	31	2.5	0.76	33
3.50	80	31.2	15	0.9	0.85	21	45	29.1	40	2.2	0.80	24
4.0	234	32.1	5	1.5	0.87	22	63	31.2	67	0.6	0.90	6
5.0							95	35.0	83	0.4	0.89	17
7.50							140	39.1	84	0.6	0.86	16
10.0							157	41.4	86	0.6	0.84	14

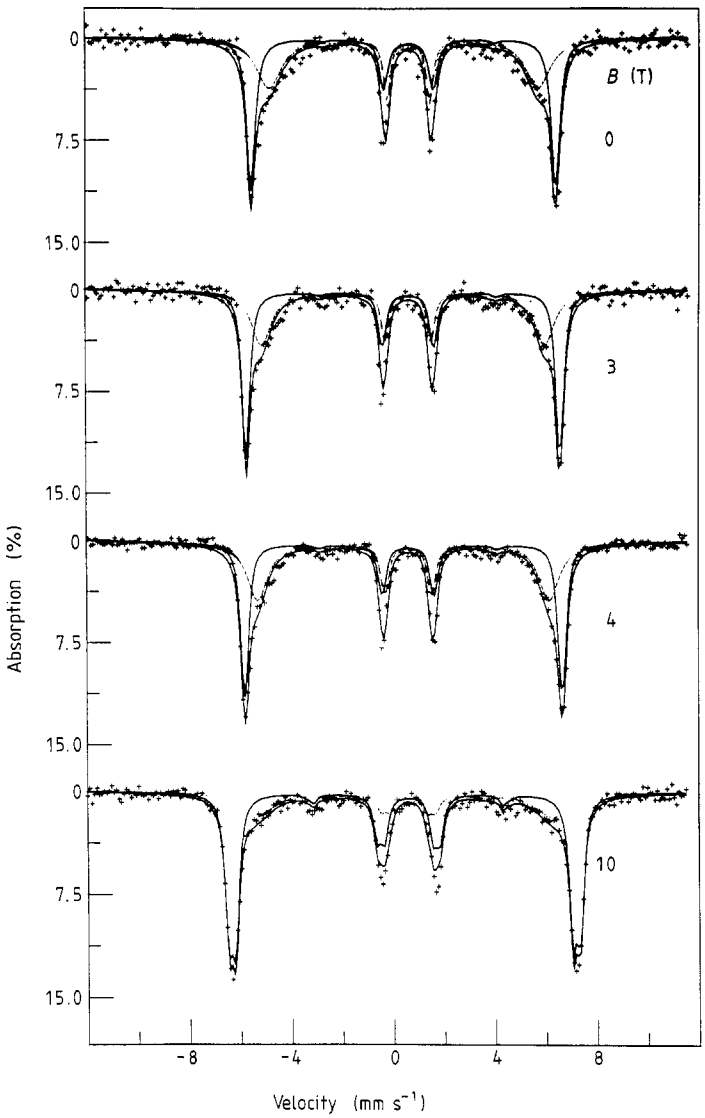

Figure 8. Series of spectra with field B applied along the crystal c axis in the single-crystal sample of $K_2Fe_{0.99}Ga_{0.01}F_5$ showing no field-induced broadening. The fits to the data are computed as discussed in § 3.3.

strengths was measured to be $J'/J = 9 \times 10^{-4}$ and the ratio of anisotropy to exchange fields to be $B_A/B_E \sim 8.5 \times 10^{-4}$ (Cooper *et al* 1982b). In the doped material the non-magnetic Ga^{3+} ions substitute for the Fe^{3+} ions in the magnetic chains. The effect of such doping will be to weaken greatly the magnetic interaction between Fe^{3+} ions on each side of the Ga^{3+} ion; thus the Ga^{3+} ions separate the Fe^{3+} chains into segments that couple weakly to each other along the chain direction and weakly—through the J' exchange coupling—to neighbouring chains. It is the coupling of the chain segments to give a magnetically ordered state at T_N and, at temperatures $T < T_N$, the fluctuation of chain segments within an ordered state giving rise to relaxation spectra that form the basis of the magnetic model.

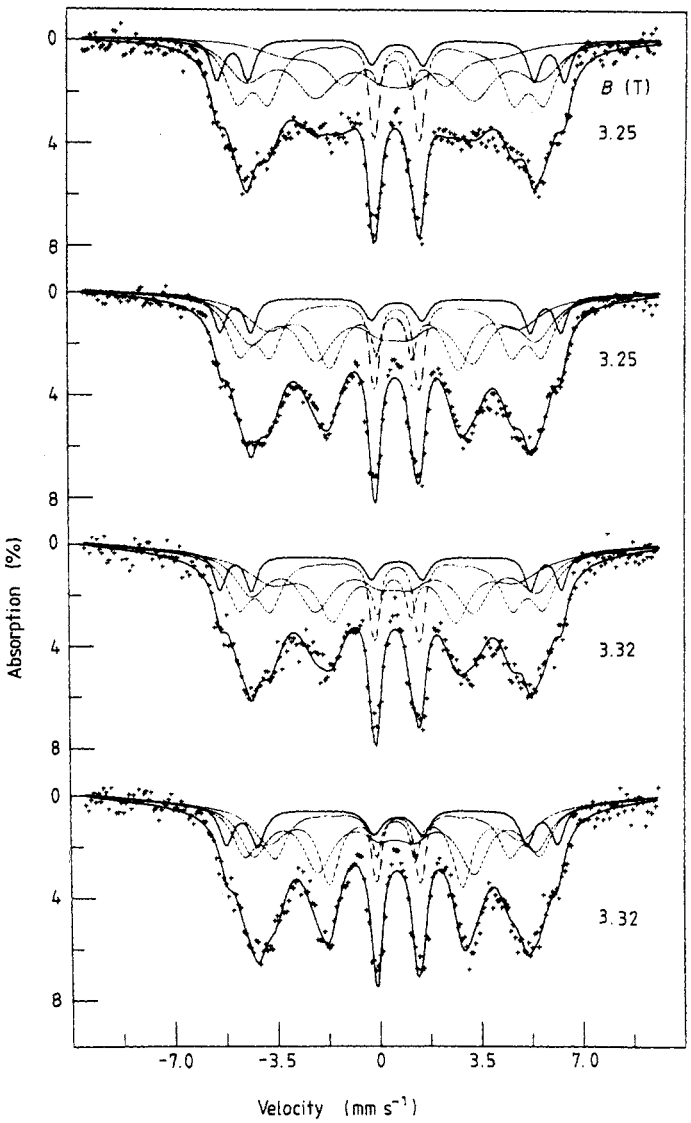

Figure 9. Spectra taken at 4.2 K near the spin-flop transition of applied fields $B = 3.19$ T and $B = 3.25$ T in a sequence of increasing field and $B = 3.19$ T and $B = 3.25$ T in a sequence of decreasing field to illustrate hysteresis in the spin-flop transition. The fits to the spectra are computed as discussed in § 3.3.

4.2. Evolution of spectra with increasing temperature

For all values of doping level x the series of spectra taken with increasing temperature (figures 2–4) show a similar progression of sharp sextet, broadened magnetic component with doublet to sharp doublet. The fits are composed of the three components listed in table 1. At the lower temperatures it is thought that component 1 represents the fast fluctuation of ions within effectively non-relaxing segments of magnetic chains which give rise to the values of the relative magnetisation M, while component 2 reflects the relaxation of segments. This distinction is lost as the temperature approaches T_N. The doublet component which can only arise from fast-fluctuating ions not subject to an

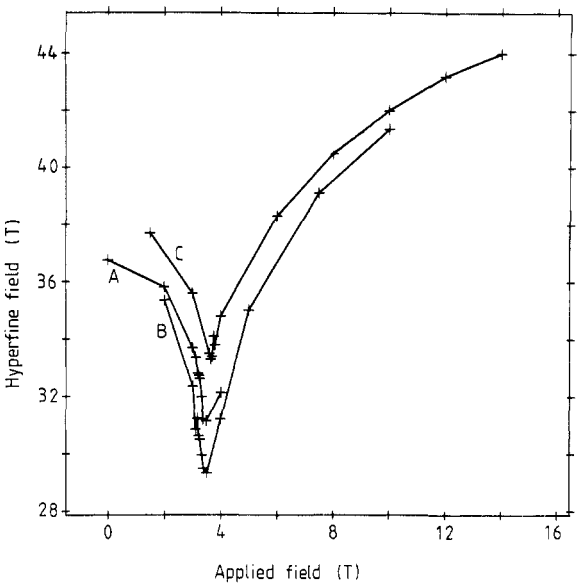

Figure 10. Variation of hyperfine field B_{hf} with applied field B at 4.2 K for (A) the antiferromagnetic phase and (B) the spin-flop phase ion $K_2Fe_{0.99}Ga_{0.01}F_5$ and (C) for the antiferromagnetic and spin-flop phases of K_2FeF_5. The curves through the points are to guide the eye.

external field is negligible until a few tenths of a degree below T_N. The rise in intensity of this component near T_N is thought to be due to temperature or sample inhomogeneities giving rise to non-magnetic regions. At temperatures greater than T_N fast relaxation in zero field gives rise to the observed sharp doublet spectra.

4.3. Variation of ordering temperature T_N with x

The theory of ordering in a material composed of segmented quasi-one-dimensional magnetic chains is adapted from the treatment of ordering in analogous undoped systems (Imry *et al* 1975, Villain and Loveluck 1977). In the undoped system the correlation length ξ of coupled spins S within the chains at a temperature T is given by

$$\xi(T) = 2JS(S+1)/kT \tag{1}$$

and the ordering temperature T_N by

$$kT_N = 4zJ'\xi(T_N)S(S+1)/3 \tag{2}$$

where z is the number of nearest-neighbour chains. In the doped material the correlation length is limited by the non-magnetic atoms as well as by thermal excitations. For a doping level x the correlation length $\xi(x, T)$ can be written

$$1/\xi(x, T) = 1/\xi(T) + x \tag{3}$$

which leads to a correlation length at T_N in a material of doping level x given by

$$\xi(x, T_N) = 2JS(S+1)/[kT_N + 2JS(S+1)x]. \tag{4}$$

Substitution of equation (4) into equation (2) gives a quadratic relation for T_N which, for a value of $S = \frac{5}{2}$ for the Fe^{3+} ions, can be written

$$T_N = -35mx/4 + [(35mx/4)^2 + 2450mn/16]^{1/2} \tag{5}$$

where $m = J/k$ and $n = 4zJ'/3k$.

This dependence of T_N upon x was fitted to the experimental points of figure 6 with m and n as variable parameters. It is seen that the shape accounts well for the experimental dependence. The values of the best-fit parameters were $J/k = 15$ K and $4zJ'/3h = 2.3 \times 10^{-2}$ K which, for a value of $z = 4$ gives a ratio of $J'/J = 3 \times 10^{-4}$. These values are of the same order as the values $J/k = 9.5$ K and $J'/J = 9 \times 10^{-4}$ determined (Cooper *et al* 1982b) for the pure material.

4.4. Spin-flop transition

In pure K_2FeF_5 the spin-flop transition occurs at $B_{sf}(0) = 3.65 \pm 0.1$ T with coexistence of the phases over the range of applied field $3.60 < B < 3.75$ T. In this range of field increased line widths were observed in the spectra; the greatest occurred at $B = B_{sf}$ and was about 2.5 times the natural width. No hysteresis was observed (Pankhurst *et al* 1985).

The series of spectra in figure 7 that illustrate the spin-flop transition in the single crystal of $K_2Fe_{0.99}Ga_{0.01}F_5$ at 4.2 K show that relaxation broadening has begun by an applied field $B = 2$ T and becomes very great over the region $3 < B < 4$ T before narrowing of the lines occurs for $B > 5$ T.

A field B applied along the antiferromagnetic axis gives rise to an energy term $-\frac{1}{2}\chi B^2$ which acts to cancel the crystalline anisotropy K. At spin flop,

$$K - \tfrac{1}{2}\chi_{\parallel} B_{sf}^2 = -\tfrac{1}{2}\chi_{\perp} B_{sf}^2$$

or

$$B_{sf} = [2K/(\chi_{\perp} - \chi_{\parallel})]^{1/2} = (2B_E B_A)^{1/2}$$

where $B_A = K/M$, $B_E = M/\chi_{\perp}$ and M is the sublattice magnetisation.

In the model of weakly coupled segments of strongly coupled spins the crystalline anisotropy of the segment increases with segment length. As the field is increased from zero the shorter lengths have their anisotropy cancelled first. This causes them to fluctuate giving rise to a broadened spectrum component and to undergo spin flop. As the field increases in the range $2 < B < 4$ T longer and longer chain segments behave similarly giving rise to large broadening of the spectra components and coexistence of phases. At fields $B > 5$ T the increasing net anisotropy $(-\frac{1}{2}(\chi_{\perp} - \chi_{\parallel})B^2 + K)$ causes a decrease in fluctuations leading to a narrowing of lines in the spin-flop phase spectrum. The model thus accounts naturally for the line broadening about spin flop and for the fact that some intensity of the spin-flop component enters the spectra at fields as low as $B = 2$ T although the main spin-flop field B_{sf} is considerably higher.

The value of the spin-flop field is determined from figure 10 to be $B_{sf}(0.01) = 3.4 \pm 0.1$ T. This value can be related to the spin-flop field for pure K_2FeF_5, $B_{sf}(0)$, by the expression (Breed *et al* 1973)

$$B_{sf}(0.01) = B_{sf}(0) \times 0.99\ (T_N(0.01)/T_N(0))^{1/2}.$$

Using the value of $T_N(0.01) = 6.1$ K determined above, the expression predicts $B_{sf}(0.01) = 3.4$ T, in excellent agreement with the measurements.

Spin-wave theory predicts hysteresis of the spin-flop transition

$$B_{sf}^{\uparrow} - B_{sf}^{\downarrow} = \Delta B_{sf} = B_{sf}(B_A/B_E)$$

which is unobservably small in pure K_2FeF_5. In the doped sample this expression predicts if anything less hysteresis than in the pure material. Thus the hysteresis experimentally observed in figure 9 which occurs over a range of field $3.19 < B < 3.38$ T cannot be explained by spin-wave theory and must be due to some different mechanism.

In summary the spectra of the doped antiferromagnets $K_2Fe_{1-x}Ga_xF_5$, the evolution of the spectra with temperature and applied field, the variation of the ordering temperature T_N with doping level x and the value of the spin-flop field $B_{sf}(0.01)$ are qualitatively and in many cases quantitatively accounted for by a model of segments of magnetic chains with weak exchange coupling between segments and anisotropy which increases with segment length.

Acknowledgments

We wish to acknowledge the support of SERC research studentships for JC and JAJ and a Liverpool University Research Fellowship for DHJ.

References

Blume M and Tjon J A 1968 *Phys. Rev.* **165** 446–56
Breed D J, Gilijamise K, Sterkenberg T W E and Miedema A R 1973 *Physica* **68** 303–14
Cooper D M, Dickson D P E and Johnson C E 1982a *J. Phys. C: Solid State Phys.* **15** 1025–33
Cooper D M, Gupta G P, Dickson D P E and Johnson C E 1982b *J. Phys. C: Solid State Phys.* **15** 3391–9
Dance J M, Soubeyroux J L, Sabatier R, Fournes L, Tressaud A and Hagenmuller P 1980 *J. Magn. Magn. Mater.* **15–18** 534–6
Gupta G P, Dickson D P E and Johnson C E 1978 *J. Phys. C: Solid State Phys.* **11** 215–25
—— 1979 *J. Phys. C: Solid State Phys.* **12** 2419–21
Imry Y, Pincus P and Scalapino D 1975 *Phys. Rev.* B **12** 1978–80
Pankhurst Q A, Johnson C E and Thomas M F 1985 *J. Phys. C: Solid State Phys.* **18** 3249–53
Villain J and Loveluck J M 1977 *J. Physique* **38** L77–80